Template-Directed In Crystallo Photopolymerization of a Donor–Acceptor Cyclopropane: When Everything Falls into Place!

Michel Giorgi, Kévin Masson, Sara Chentouf, Laurent Commeiras, Paola Nava, Gaëlle Chouraqui

Template-Directed *In Crystallo* Photopolymerization of a Donor−Acceptor Cyclopropane: When Everything Falls into Place!

Michel Giorgi,* Kévin Masson, Sara Chentouf, Laurent Commeiras, Paola Nava,* and Gaëlle Chouraqui*

ABSTRACT: A single-crystal-to-single-crystal solid-state reaction of vinylogous donor−acceptor cyclopropanes is documented. The enantiospecific synthesis of new products, distinct from those obtained in solution, is achieved for the target compounds. Photopolymerization occurred upon X-ray exposure to the crystals. Notably, in one case, this reactivity exhibits selectivity since an ordered arrangement of polymers and unreacted cocrystallized monomeric conformers has been observed. Structural characterization of the complete transformation monitored through single-crystal X-ray diffraction and supported by molecular dynamics simulations sheds light on the subtle role of crystal packing in the reaction process. Moreover, the X-ray diffraction (XRD)-resolved structure of a donor−acceptor cyclopropane intermediate reveals an elongation in bond length that corroborates the existence of the so-called "push−pull effect".

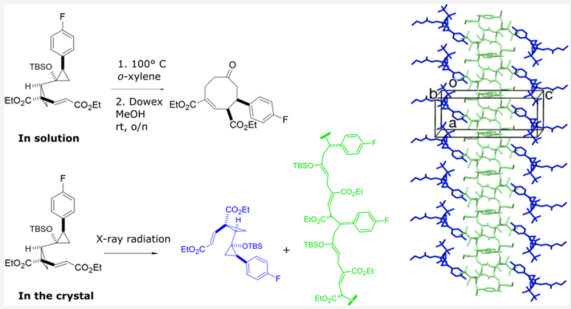

INTRODUCTION

Reactivity in crystals proves to be a powerful tool when chemical phenomena can be initiated *in situ*; it becomes possible to characterize structurally and finely, on the same sample, the initial and final steps of the process and sometimes even the reaction intermediates. While this is well established for biological crystals, numerous reactions have also been documented on porous crystals (such as host−guest compounds, MOFS, cryptants, etc.) and on dense organic/inorganic phases.[1−9] The most frequently observed reactivity remains polymerization, facilitated by the stacking of precursors, the suitable orientation of the reaction sites, and the dynamic nature of molecules in crystals[10]—a phenomenon known as topochemical polymerization.[11−18]

In the realm of topochemical photopolymerization, single-crystal-to-single-crystal (SCSC) transformations present a unique avenue and offer distinct advantages over liquid-state reactions. SCSC transformations ensure precision, preserving the original crystal structure and minimizing environmental impact.[18−20] The solid-state nature reduces reliance on solvents, simplifying purification and enhancing our understanding of reaction mechanisms and kinetics. Specific reactions that may be inaccessible through conventional solution-phase synthesis can be achieved in the solid state.[11,22−24] Moreover, they can be directed toward the formation of different products than those obtained in solution.[19−21,25] This approach, alongside its application in various crystal systems, stands as a promising strategy for advancing precise synthesis in materials science.[26−30]

In this study, we present the structural analysis of a series of donor−acceptor cyclopropane (DAC) molecules and their crystal-to-crystal transformation, revealing differences in reactivity between the solid state and in solution. We characterized an unexpectedly selective photopolymerization of one of the two cocrystallized conformers in a crystal using X-rays. To the best of our knowledge, there are only two known cases of a comparable phenomenon: a photopolymerization involving two out of three cocrystallized monomers[31] and a cyclization involving one out of two cocrystallized monomers.[32,33] The comparison of the crystal packing of different compounds within the family, supported by molecular dynamics (MD), highlights the role of the crystal's plasticity in the reaction process. Thus, we demonstrate that crystal packing influences reactivity and that the framework constraints act as a reaction parameter, guiding the formation of nanostructures through the stereoisomerically controlled self-sorting assembly.

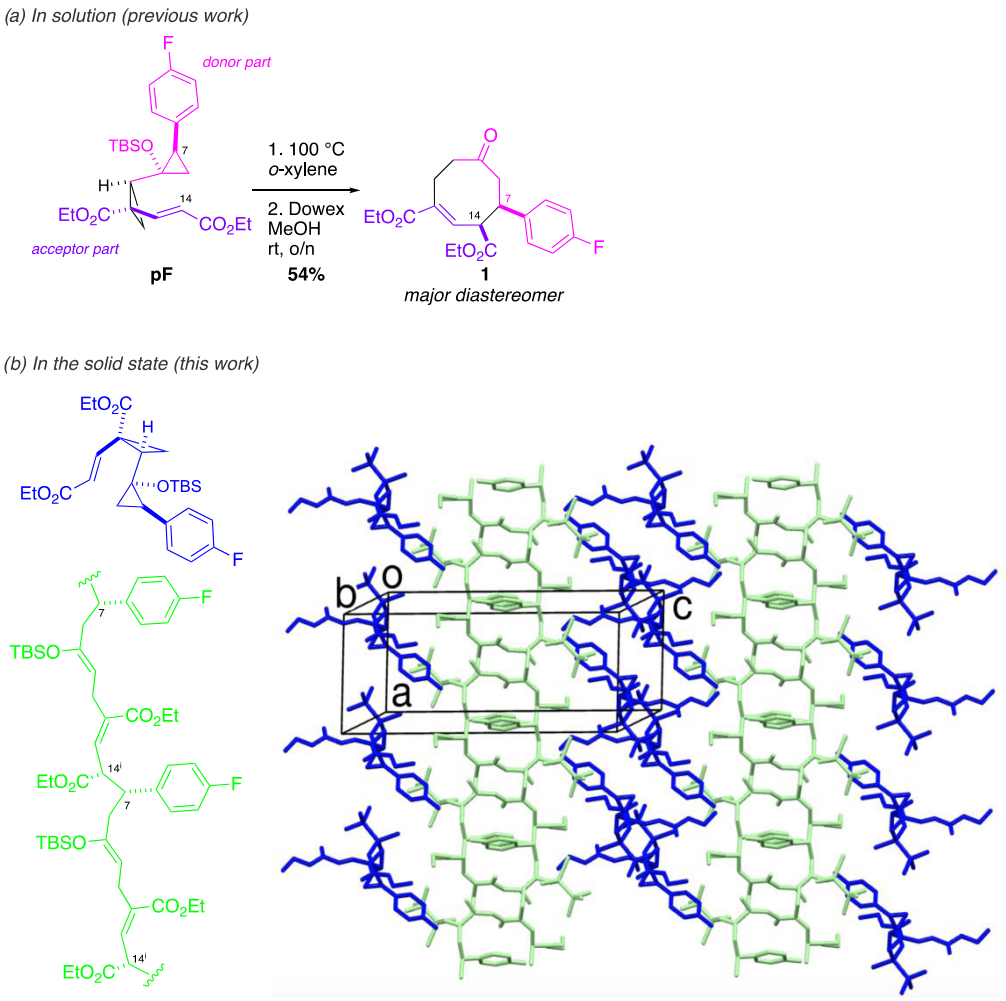

Figure 1. Solution-phase reactivity (a) *vs* solid-phase reactivity (b) of vinylbiscyclopropane **pF**. In (b), the nonactive monomers and the polymers are colored blue and green, respectively.

DACs represent extraordinary chemical structures.[34−39] Accordingly, the opposing electronic characteristics of neighboring substituents, coupled with the inherent ring strain of the cyclopropane (around 27.5 kcal·mol^{-1}), not only guide but also ease the process of bond cleavage.[40,41] In this context, our research contributes to the ongoing exploration and understanding of the "push−pull" dynamics of DACs.

RESULTS

Through conventional solution-phase synthesis, the in-house vinylogous DAC derivatives efficiently produced the corresponding challenging all-carbon eight-membered rings with dia- and regioselectivity.[42] Typically, a solution of DAC **pF** in *o*-xylene at 100 °C selectively afforded the cyclooctenone **1** (Figure 1a). A careful selection of substituents and control of the relative stereochemistry on the starting material resulted in a substrate prone to thermal rearrangement without requiring any catalyst or reagent.

To secure the structure and the stereochemistry of the precursor **pF** in the synthesis of the cyclooctenes (Figure 1), we crystallized and measured by single-crystal X-ray diffraction (SCXRD), the racemic DAC derivative **pF** at room temperature using Cu radiation. Interestingly, we promptly observed broadening and splitting of the diffraction spots after a few minutes of irradiation, but as the crystal kept diffracting, we decided to complete the measurement and successfully solved the structure. An unexpected and unique feature emerged: the final crystal packing exhibited a structure with alternated layers of **pF** monomers and of a polymeric structure resulting from the reaction between adjacent monomers (Figure 1b).

We thus decided to investigate the reaction process in the crystalline state and measured first a new sample at a lower temperature (150 K). In contrast to the previous experiment, the final resolution of the crystal, **pF-150 K**, showed the presence of two independent monomeric conformers in the asymmetric unit: **pF-m** and **pF-p** (Figure 2a). A comparison of both conformers shows that they are almost superimposable, with a root-mean-square deviation of 0.33 Å considering all non-H atoms. The main difference between them arises from a rotation of approximatively 65° of the terminal CH_2−CH_3 substituent of the vinyl ester (see Figure S1). Expanding the crystal packing along the direction of the previously detected

(a) SCXRD of **pF** at 150 K

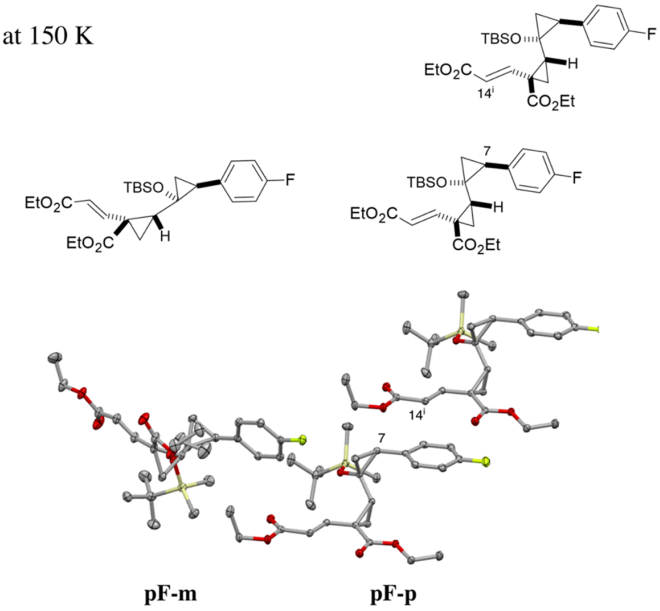

(b) SCXRD monitoring of the photopolymerization of **pF-p** monomer of **pF**

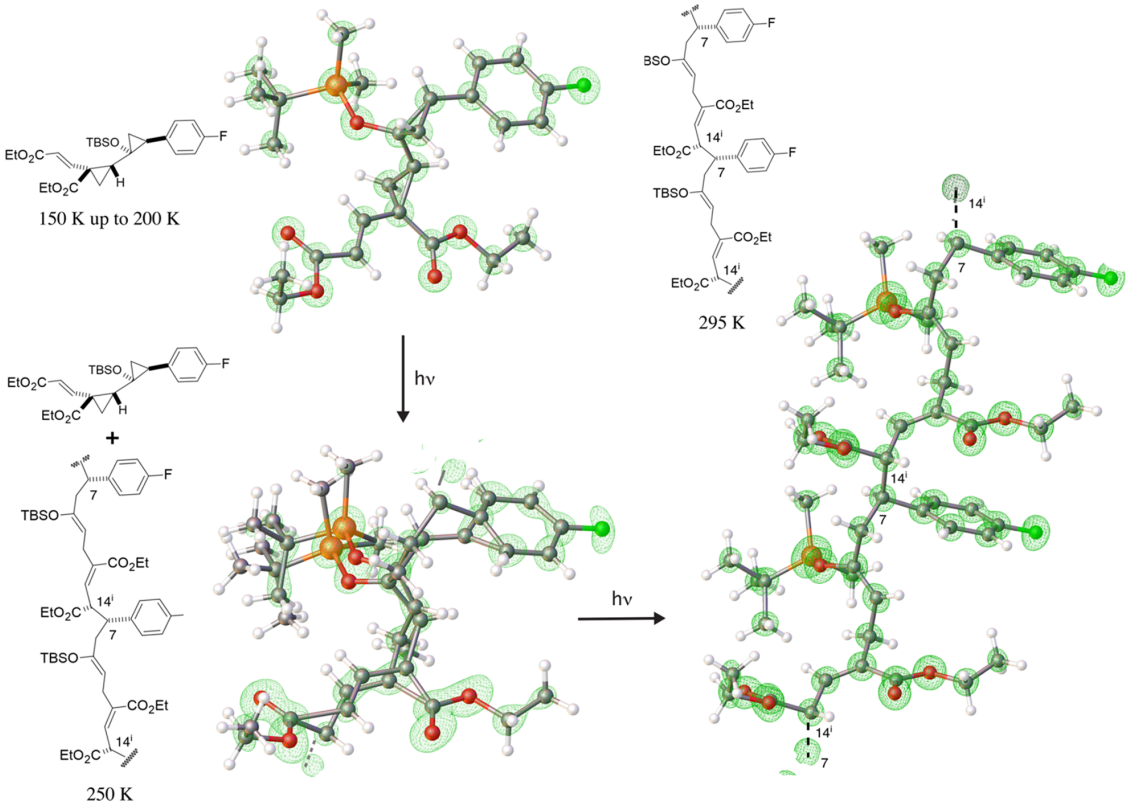

Figure 2. SCXRD observation **of pF** at different temperatures. (a) At 150 K showing the **pF-m** monomer and two adjacent proactive monomers **pF-p**. (b) Structures of **pF-p** in ball and stick and electron-density maps (contour level of 1.5 e/Å^3) are shown for measurements at 150−200 K (top left), 250 K (bottom left), and 296 K (right: only two monomers of the polymer are represented).

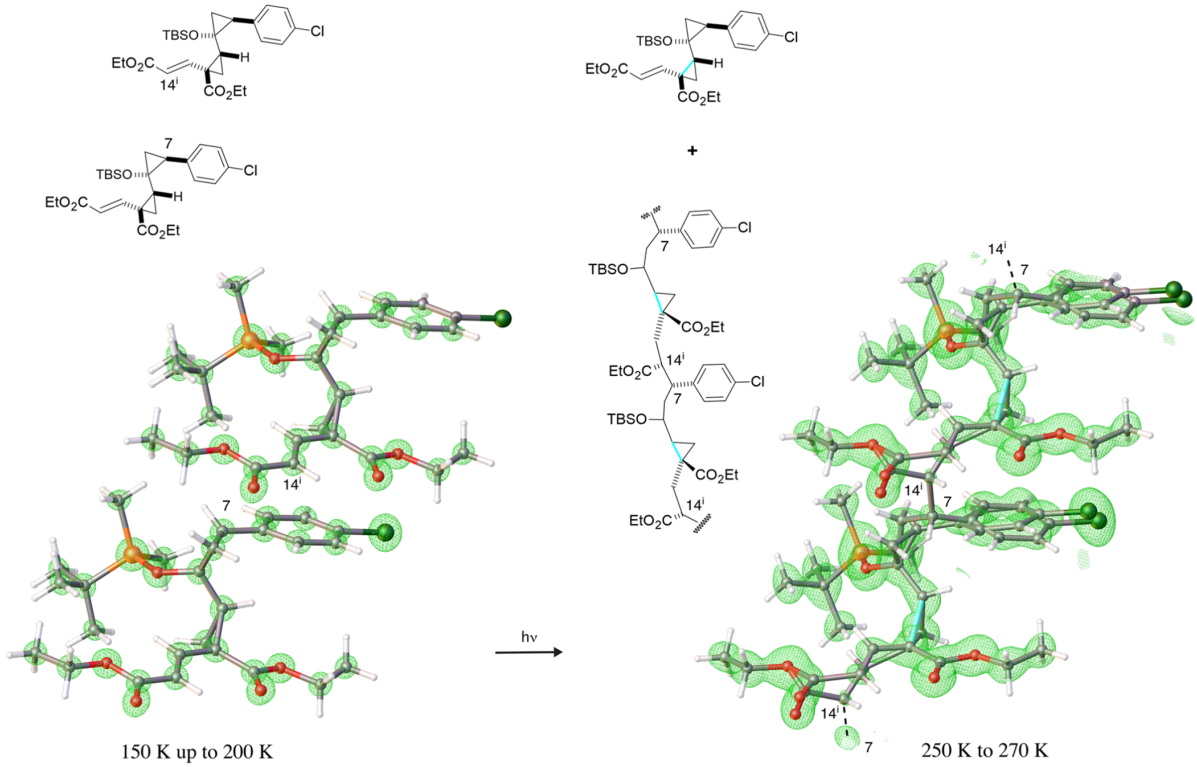

Figure 3. SCXRD observation **of pCl** at different temperatures. The structures in ball and stick and electron-density maps (contour level of 1 e/Å^3) are shown for measurements at 150−200 K (left) and at 270 K (right: only two monomers of the polymer are represented). The elongated inner C−C bond of the cyclopropane is colored blue.

polymerization (crystallographic axis **a**, Figure 1b), we also observed that the **pF-p** monomers were nicely oriented, facilitating topochemical polymerization among all identical subunits of the crystal cells (Figure 2a). Indeed, the two mean planes containing the substituents of the active sites, *i.e.*, the benzylic carbon C7 and the *para*-fluorobenzene, and the vinyl ester from the adjacent symmetrically related molecule *i* (symmetry code *i*: $-1 + x, y, z$), are almost parallel with an angle of about 2°. Moreover, the distance between the two reactive carbons C7 and C14^i is equal to 4.324(2) Å.

Measurements at 200, 250, and 295 K were then performed on the same sample and revealed that no reaction occurred up to 200 K. At 250 K, we observed a change in the diffraction pattern once again, accompanied by a slight but significant modification of some cell parameters and an approximately 5% increase in the unit cell volume (see Table S1). Subsequently, all structures were solved and refined, enabling us to capture some snapshots of the reaction process (Figure 2b).

In every measurement, the **pF-m** conformer remains unaffected by irradiation. However, at 250 K, the cocrystallized conformer **pF-p** initiated a reaction. The structure reveals the presence of a mixture of the precursor and an intermediate of the reaction sharing the same site, each with an occupation factor of 0.5 (Figure 2b left). In the intermediate, the two cyclopropane rings have opened. The C14^i carbon atom of the reacting vinyl ester adopts a pyramidal conformation, characteristic of sp^3 hybridization. Additionally, the *para*-fluorobenzene plane is distorted toward a half-chair conformation to bring the reacting C7 carbon closer to the neighboring unit, resulting in a shortened distance of C7−C14^i to 1.63(1) Å (see Figure S2). At 295 K, the regio-, diastereo-, and enantiospecific reactions are completed, and the **pF-p** site is fully occupied by the final polymer (Figure 2b right and Figure S3). The remarkable ability of the DAC **pF** compound to selectively react within the crystal is attributed to the specific molecular-packing structure, wherein two conformers cocrystallize to form alternating nanolayered structures. This arrangement suggests that the first layer of the nonreacting conformer acts as a template or stabilizing matrix, thus enabling the second one to undergo the reaction (Figure 1b).[32,33]

We also tested other activation sources, including SCXRD using Mo radiation, ultraviolet−visible (UV−vis), laser, or microwaves, to attempt polymerization of our compound. However, none of these approaches proved successful as no crystal transformation was observed (see the Supporting Information (SI)). Additionally, the wavelength and intensity of the X-ray source emerged as crucial factors influencing the reactivity (see the SI).

To investigate whether the nature or position of the halogen atom on the benzene ring could influence the outcome of the polymerization, we examined the behavior of the *para*-chlorobenzene and *meta*-fluorobenzene DAC derivatives using Cu radiation.

The crystal structure of the *para*-chlorobenzene DAC derivative, **pCl**, at 150 K, showed the presence of only one conformer in the asymmetric unit, which was positioned favorably for topochemical polymerization, with a distance of

(a) The **pF** (i) SCXRD structure at 150 K and (ii) and (iii) bulk simulation structures at 150 K and 300 K, respectively.

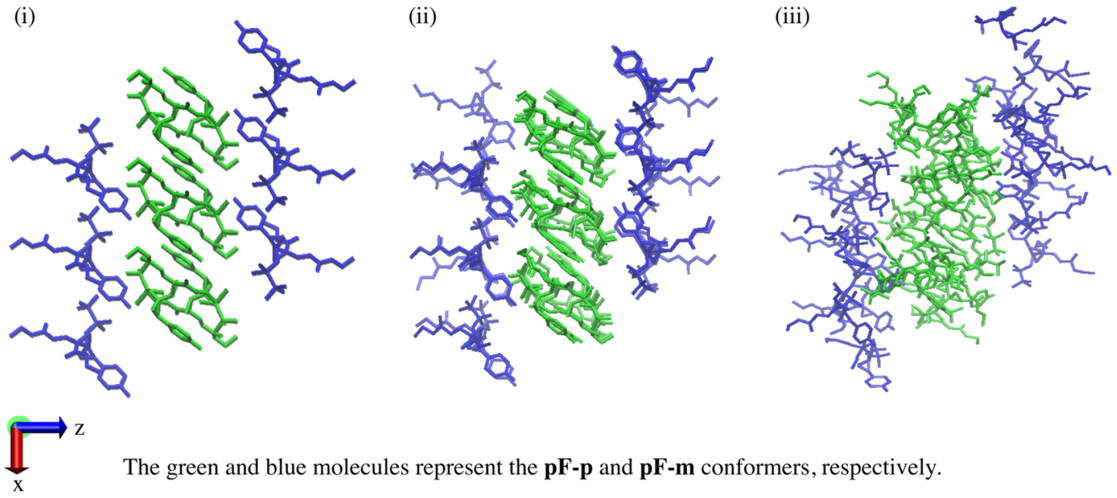

The green and blue molecules represent the **pF-p** and **pF-m** conformers, respectively.

(b) y and z components of the average displacements for **pF-p** and **pF-m** conformers along MD trajectory at 300 K.

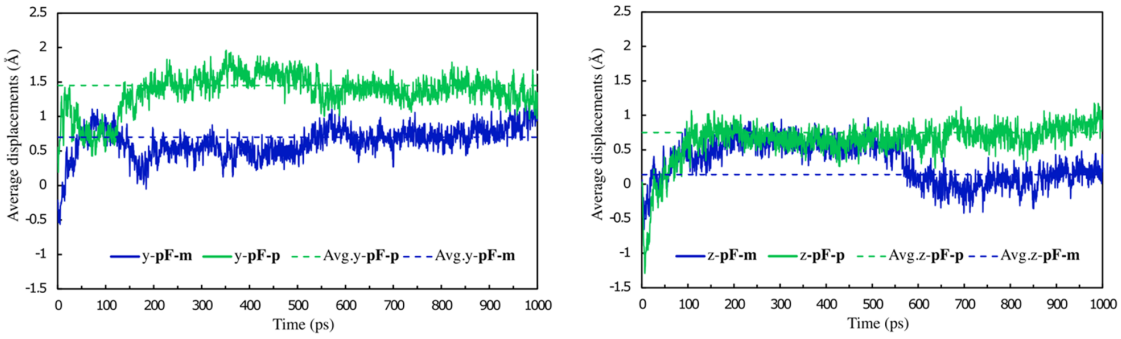

(c) The **pCl** (i) SCXRD structure at 150 K and (ii) and (iii) bulk simulation structures at 150 K and 300 K, respectively.

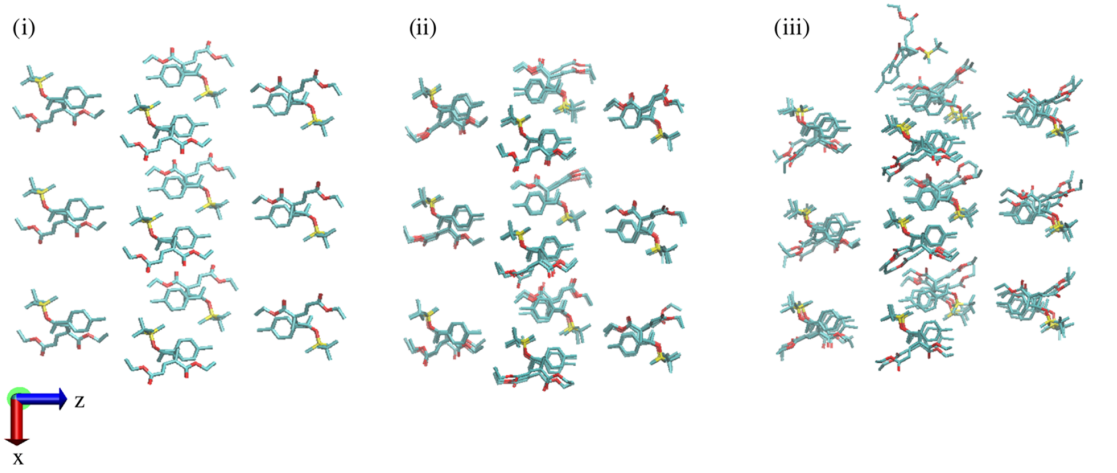

Figure 4. Molecular dynamics on **pF** and **pCl**.

4.118(2) Å between the two reactive carbons. No significant changes were observed up to 200 K as in the case of **pF** (Figure 3). However, at 250 K, a mixture of two reaction intermediates was observed in a 2/3:1/3 ratio. In the major

occupied site, the structure revealed an elongation of the inner C−C bond of the cyclopropane ring linked to the alkene moiety with a length of 1.713(9) Å, which is the bond of the donor−acceptor cyclopropane involved in the "push−pull" effect.[43] In the minor occupied site, this cyclopropane ring remained closed, with the same elongated bond as in the major one, but the cyclopropane ring connected to *para*-chlorobenzene was fully opened. Moreover, polymerization along the crystallographic axis **b** was completed, and the DAC monomers are all linked together with a C−C bond distance equal to 1.56(2) Å (see Figure S6). At 270 K, the process continued with a mixture of the two intermediates sharing the same site, each with an occupation factor of 0.5. For the first bond, the inner bond of the cyclopropane ring linked to the alkene is further elongated to 1.87(1) Å. The second intermediate exhibited the same structural characteristics as in the sample measured at 250 K but in a greater proportion (50%), indicating an ongoing transformation. Finally, measurements were no longer feasible at 290 K as the sample lost its crystallinity.

We pursued our study by focusing on the *meta*-fluorobenzene derivative, **mF**. Unlike **pF**, its crystal structure at 150 K showed the presence of only one conformer in the asymmetric unit (see Figure S7). Despite the DAC molecules appearing to be in a favorable position for topochemical polymerization (the distance between the proactive carbons is only 3.613(4) Å), no reaction occurred at higher temperatures.

In summary, the three derivatives, all favorably oriented for a topochemical reaction, exhibited different behaviors under irradiation. Polymerization kept the crystal intact in the case of **pF** but with a selective reactivity on only one of the two cocrystallized conformers. For **pCl**, polymerization led to the destruction of the crystal, and no polymerization occurred for **mF**. The polymerizing crystals responded similarly to the stress induced by the reaction process by twinning and expanding their unit cell volume by about 5% for **pF** and 8% for **pCl** (see Tables S1 and S2). The examination of other polymorphs, as well as other halogen-substituted and non-halogen-substituted DACs, reveals that no polymerization occurs (see the SI for more details) since they are not oriented in a position favorable for topochemical polymerization. The same holds true for each separated enantiomer of the **pF** DAC, meaning that the enantiopurity clearly influences the packing of the crystal.

To conclude, based on initial experimental and observational data, the most noteworthy aspect here is that polymerization and crystal integrity in the **pF** case are closely tied to both the chirality of the monomer/conformer pair and their packing process. The stereoisomerically supramolecular structure controls the self-sorting assembly. In other words, the chirality of the supramolecular edifice drives the formation of the nanostructure.

DISCUSSION

To delve deeper into understanding the phenomena influencing the distinct reactivity of the three crystal phases described above, we conducted computational theoretical studies examining the role of (i) the nature and position of the halogen atom and (ii) the crystal packing.

We first computed a pathway at the density functional theory level in the gas phase for **pF**, **pCl**, and **mF** to propose a plausible mechanism for the formation of the C−C bond between two monomers. However, the results showed substantial equivalence in terms of barrier and reaction energies and could not justify their distinct behaviors (see the SI). This suggests that the differences are related to the constraints imposed by the packing in the crystal and their dynamic behavior. This last outcome prompted us to further analyze and compare the packing in the crystals. However, examination of the packing of the three crystals through Hirshfeld surface analysis[44,45] and void detection did not reveal major differences (see Figures S12−S15). Molecular dynamics (MD) simulations, on the other hand, enable the examination of the dynamic properties of microscopic systems and the exploration of molecular details that cannot be assessed through real experiments. Therefore, we conducted MD studies to track the movement of the molecules. While these calculations do not capture bond breaking and formation, they allow the evaluation of the physical motion of atoms and molecules in the crystals during the early stage of polymerization. MD simulations were conducted on the **pF**, **mF**, and **pCl** crystals using GROMACS[46] © software with GAFF[47] force field (SI for details). We initially determined the equilibrated volumes at two different temperatures, 150 and 300 K. The calculated volume expansions ΔVth from 150 to 300 K are in very good agreement with those observed experimentally in the three crystals (computed values are 4.88, 0.12, and 8.5% compared to 5.32, 0, and 8.39% in the measured **pF**, **mF**, and **pCl** crystals, respectively).

To illustrate the molecule displacements within the crystals, Figure 4a,c presents the SCXRD structures obtained at 150 K, alongside the snapshot pictures of the equilibrated structures after 1 ns MD simulations at 150 and 300 K, for **pF** and **pCl** crystals, respectively. The crystalline order is maintained for the **pCl** structure during the MD simulations, while greater plasticity emerges for the **pF** structure. Additionally, we observe that the plasticity appears to be more significant in the zone corresponding to the **pF-p** conformers (in green). On the other hand, there are almost no movement observed for **mF** (see the SI).

To appreciate and quantify the dynamic behavior of the **pF-m** and **pF-p** conformers within the crystal, displacements between the adjacent molecules stacked along the polymerization axis were calculated along the MD trajectory (Figure 4b) at 300 K, using the geometrical centers of the molecules as reference points. The movements along all three coordinates were analyzed. Only the *y* and *z* components (**b** and **c** unit cell directions in the crystals) are presented here as the *x* direction component is nearly zero. These displacements are more significant for **pF-p**: indeed, the time-averaged value along y (removing the first 200 ps MD) is twice as significant for the **pF-p** conformer (1.45 Å) than for **pF-m** (0.7 Å). We observed the same trend along the *z* direction (0.75 Å for **pF-p** and 0.14 Å for **pF-m**). The average displacements of the geometrical centers of the **pCl** molecule were also calculated for comparison (see the SI), and it can be noted that the displacements are almost zero along the *x* and *z* directions and of the order of 1 Å along the y direction (*y* being the direction of polymerization of **pCl-250 K**).

Based on these calculations and observations, it becomes evident that the position and orientation of the topochemical polymerization precursors are necessary but not sufficient to sustain the reaction after the opening of the cyclopropane rings. Some degrees of freedom are necessary, and in the case of **pF**, the required movements occur in the plane perpendicular to the direction of polymerization. Moreover,

this plasticity enables the crystal to maintain a certain level of integrity. In the case of **pCl**, the movement is limited to the direction of polymerization, and the insufficient free space in the perpendicular direction results in the ultimate destruction of the crystal lattice. As far as our knowledge extends, the utilization of molecular dynamics (MD) in comprehending the crystal-to-crystal transformations has been notably scarce within purely organic systems.[48−50]

CONCLUSIONS

Solid-state synthesis provides an exceptional reaction microenvironment that yields reactivity distinct from that of conventional solution-phase methods. This solid-state polymerization presents a stark contrast to the bulk-solvent intramolecular reactivity, allowing for the formation of molecular complexity not previously attained. Particularly noteworthy is the enantiospecific transformation of only one cocrystallized conformer in the *para*-fluoro derivative case, leaving the second intact—a rarity with only two reported instances in the literature. This observation underscores the significant influence of the crystalline environment on the chemical reactivity.

Structural analysis using SCXRD revealed the necessity of a topochemical arrangement of molecules to initiate the polymerization process. However, this alone proved insufficient, and molecular dynamics further illustrated that polymerization necessitates crystal plasticity. This grants molecules the freedom to expand and allows for the opening of the cyclopropane rings and ensuing reactivity. This utilization of MD in our study is particularly noteworthy as it is uncommon to employ such simulations in systems of this nature.

Moreover, our findings with the *para*-fluoro derivative demonstrate that the first layer of the nonreacting conformer functions as a crucial template, ensuring crystal integrity and stabilizing the matrix. Exposure to the constraints of the framework influences both stability and reactivity; thus, the molecular edifice can be considered as an additional reaction condition, akin to classical factors such as temperature or pressure, for example.

The combined use of SCXRD to monitor reaction transformations and MD simulation provided a detailed understanding of the reaction mechanisms at the atomic scale.

SCSC chemical reactions, initiated and monitored through X-rays, provide valuable snapshots capturing the interplay between reactive sites. They can give access to reaction intermediates within the solid crystalline state. In this case, data collected during the topochemical polymerization process of the *para*-chloro derivative offered interesting perspective from a fundamental point of view. For the first time, we could visualize the so-called "push−pull effect" imparted by the neighboring donor and acceptor substituents on the cyclopropane, with all of the precautions that need to be taken with interpretations based solely on SCXRD.[51,52]

Topochemical reactions are intricately tied to the molecular packing within the crystal lattice and, consequently, to the proximity and proper orientation of the reactive groups. Unlike traditional chemical reactions, which primarily hinge on the chemical structure, topochemical reactions are heavily influenced by the crystallization process of a molecule. Predicting such reactions solely based on chemical composition remains an elusive objective. However, the utilization of structurally constrained molecules, such as cyclopropane substituted by two electronically antagonistic substituents, can significantly enhance the likelihood of bimolecular reactions in the solid state by facilitating strain release provided that the aforementioned prerequisite parameters (proximity, orientation, and plasticity) are met.

Accession Codes

CCDC 2312464−2312472 and 2312498−2312505 contain the supplementary crystallographic data for this paper. These data can be obtained free of charge via www.ccdc.cam.ac.uk/data_request/cif, or by emailing data_request@ccdc.cam.ac.uk, or by contacting The Cambridge Crystallographic Data Centre, 12 Union Road, Cambridge CB2 1EZ, U.K.; fax: +44 1223 336033.

AUTHOR INFORMATION

Corresponding Authors

Michel Giorgi − *Aix Marseille Universite, CNRS, Centrale Méditerranée, FSCM, 13397 Marseille, France;* orcid.org/0000-0002-4367-1985; Email: michel.giorgi@univ-amu.fr

Paola Nava − *Aix Marseille Universite, CNRS, Centrale Méditerranée, ISM2, 13397 Marseille, France;* orcid.org/0000-0002-8909-8002; Email: paola.nava@univ-amu.fr

Gaëlle Chouraqui − *Aix Marseille Universite, CNRS, Centrale Méditerranée, ISM2, 13397 Marseille, France;* orcid.org/0000-0003-4719-137X; Email: gaelle.chouraqui@univ-amu.fr

Authors

Kévin Masson − *Aix Marseille Universite, CNRS, Centrale Méditerranée, ISM2, 13397 Marseille, France*

Sara Chentouf − *Aix Marseille Universite, CNRS, Centrale Méditerranée, FSCM, 13397 Marseille, France;* orcid.org/0000-0003-0695-7260

Laurent Commeiras − *Aix Marseille Universite, CNRS, Centrale Méditerranée, ISM2, 13397 Marseille, France;* orcid.org/0000-0003-4331-6198

ACKNOWLEDGMENTS

K.M. thanks the French Ministère de l'Enseignement Supérieur et de la Recherche (MESR) for a Ph.D fellowship. Institutional financial support from Aix-Marseille Université (AMU), the Centre National de la Recherche Scientifique (CNRS), and Centrale Méditerranée is gratefully acknowledged. M.G. is thankful to Dr. Jennifer Noble (Aix Marseille Univ, CNRS, PIIM, Marseille, France) for the tests on the OPO laser, Dr. Vasile Heresanu (Aix Marseille Univ, CNRS, CINaM,

Marseille, France) for the tests on the Cu rotating anode Rigaku 200BH, Dr. Brice Kauffmann (IECB, CNRS, INSERM, Université de Bordeaux, Pessac, France) for the tests on the Cu rotating anode Rigaku FRX MM07, and Dr. Jean-Valère Naubron (Aix Marseille Univ, CNRS, FSCM, Marseille, France) for fruitful discussions. G.C. expresses gratitude to Dr. Jean-Luc Parrain (Aix Marseille Univ, CNRS, iSm2, Marseille, France) for fruitful discussions. M.G. and G.C. also appreciate Dr. Yoann Coquerel's (Aix Marseille Univ, CNRS, iSm2, Marseille, France) attentive, relevant, and constructive review of this manuscript. This work was supported by the computing facilities of the CRCMM, 'Centre Régional de Compétences en Modélisation Moléculaire de Marseille'.

REFERENCES

(1) Fernandez-Bartolome, E.; Martinez-Martinez, A.; Resines-Urien, E.; Piñeiro-Lopez, L.; Costa, J. S. Reversible single-crystal-to-single-crystal transformations in coordination compounds induced by external stimuli. *Coord. Chem. Rev.* **2022**, *452*, No. 214281.

(2) Wahyudianto, B.; Imanishi, K.; Kojima, T.; Yoshinari, N.; Konno, T. Intermediate snapshots of a 116-nuclear metallosupramolecular cage-of-cage in a homogeneous single-crystal-to-single-crystal transformation. *Chem. Commun.* **2021**, *57*, 6090−6093.

(3) Hatcher, L. E.; Warren, M. R.; Pallipurath, A. R.; Saunders, L. K.; Skelton, J. M. Watching Photochemistry Happen: Recent Developments in Dynamic Single-Crystal X-Ray Diffraction Studies. In *21st Century Challenges in Chemical Crystallography I: History and Technical Developments*; Mingos, D. M. P.; Raithby, P. R., Eds.; Springer International Publishing: Cham, 2020; pp 199−238.

(4) Das, A.; Van Trieste, G. P.; Powers, D. C. Crystallography of Reactive Intermediates. *Comments Inorg. Chem.* **2020**, *40*, 116−158.

(5) Chaudhary, A.; Mohammad, A.; Mobin, S. M. Recent Advances in Single-Crystal-to-Single-Crystal Transformation at the Discrete Molecular Level. *Cryst. Growth Des.* **2017**, *17*, 2893−2910.

(6) Hu, F.-L.; Wang, S.-L.; Lang, J.-P.; Abrahams, B. F. *In-situ* X-ray diffraction snapshotting: Determination of the kinetics of a photodimerization within a single crystal. *Sci. Rep.* **2014**, *4*, No. 6815.

(7) Legrand, Y.-M.; van der Lee, A.; Barboiu, M. Single-Crystal X-ray Structure of 1,3-Dimethylcyclobutadiene by Confinement in a Crystalline Matrix. *Science* **2010**, *329*, 299−302.

(8) Zheng, S.-L.; Wang, Y.; Yu, Z.; Lin, Q.; Coppens, P. Direct Observation of a Photoinduced Nonstabilized Nitrile Imine Structure in the Solid State. *J. Am. Chem. Soc.* **2009**, *131*, 18036−18037.

(9) Harada, J.; Uekusa, H.; Ohashi, Y. X-ray Analysis of Structural Changes in Photochromic Salicylideneaniline Crystals. Solid-State Reaction Induced by Two-Photon Excitation. *J. Am. Chem. Soc.* **1999**, *121*, 5809−5810.

(10) For a recent example of motion in crystals, see: Raju, C.; Ramteke, G. R.; Jose, K. V. J.; Sureshan, K. M. Cascading Effect of Large Molecular Motion in Crystals: A Topotactic Polymorphic Transition Paves the Way to Topochemical Polymerization. *J. Am. Chem. Soc.* **2023**, *145*, 9607−9616.

(11) Schmidt, G. M. J. Photodimerization in the solid state. *Pure Appl. Chem.* **1971**, *27*, 647−678.

(12) Sun, C.; Oppenheim, J. J.; Skorupskii, G.; Yang, L.; Dincă, M. Reversible topochemical polymerization and depolymerization of a crystalline 3D porous organic polymer with C−C bond linkages. *Chem* **2022**, *8*, 3215−3224.

(13) Hema, K.; Raju, C.; Bhandary, S.; Sureshan, K. M. Tuning the Regioselectivity of Topochemical Polymerization through Cocrystallization of the Monomer with an Inert Isostere. *Angew. Chem., Int. Ed.* **2022**, *61*, No. e202210733.

(14) Hema, K.; Ravi, A.; Raju, C.; Pathan, J. R.; Rai, R.; Sureshan, K. M. Topochemical polymerizations for the solid-state synthesis of organic polymers. *Chem. Soc. Rev.* **2021**, *50*, 4062−4099.

(15) Mohanrao, R.; Hema, K.; Sureshan, K. M. Topochemical synthesis of different polymorphs of polymers as a paradigm for tuning properties of polymers. *Nat. Commun.* **2020**, *11*, No. 865.

(16) Guo, Q.-H.; Jia, M.; Liu, Z.; Qiu, Y.; Chen, H.; Shen, D.; Zhang, X.; Tu, Q.; Ryder, M. R.; Chen, H.; Li, P.; Xu, Y.; Li, P.; Chen, Z.; Shekhawat, G. S.; Dravid, V. P.; Snurr, R. Q.; Philp, D.; Sue, A. C.-H.; Farha, O. K.; Rolandi, M.; Stoddart, J. F. Single-Crystal Polycationic Polymers Obtained by Single-Crystal-to-Single-Crystal Photopolymerization. *J. Am. Chem. Soc.* **2020**, *142*, 6180−6187.

(17) Athiyarath, V.; Sureshan, K. M. Designed Synthesis of a 1D Polymer in Twist-Stacked Topology via Single-Crystal-to-Single-Crystal Polymerization. *Angew. Chem., Int. Ed.* **2020**, *59*, 15580−15585.

(18) Kohlschütter, V. Topochemische Reaktionen. *Helv. Chim. Acta* **1929**, *12*, 512−529.

(19) Kusaka, S.; Kiyose, A.; Sato, H.; Hijikata, Y.; Hori, A.; Ma, Y.; Matsuda, R. Dynamic Topochemical Reaction Tuned by Guest Molecules in the Nanospace of a Metal−Organic Framework. *J. Am. Chem. Soc.* **2019**, *141*, 15742−15746.

(20) Medishetty, R.; Bai, Z.; Yang, H.; Wong, M. W.; Vittal, J. J. Influence of Fluorine Substitution on the Unusual Solid-State [2 + 2] Photo-Cycloaddition Reaction between an Olefin and an Aromatic Ring. *Cryst. Growth Des.* **2015**, *15*, 4055−4061.

(21) Ariel, S.; Askari, S.; Scheffer, J. R.; Trotter, J. Latent photochemical hydrogen abstraction reactions realized in crystalline media. *J. Org. Chem.* **1989**, *54*, 4324−4330.

(22) Cuccu, F.; De Luca, L.; Delogu, F.; Colacino, E.; Solin, N.; Mocci, R.; Porcheddu, A. Mechanochemistry: New Tools to Navigate the Uncharted Territory of "Impossible" Reactions. *ChemSusChem* **2022**, *15*, No. e202200362.

(23) Seo, T.; Toyoshima, N.; Kubota, K.; Ito, H. Tackling Solubility Issues in Organic Synthesis: Solid-State Cross-Coupling of Insoluble Aryl Halides. *J. Am. Chem. Soc.* **2021**, *143*, 6165−6175.

(24) Tanaka, K.; Toda, F. Solvent-Free Organic Synthesis. *Chem. Rev.* **2000**, *100*, 1025−1074.

(25) Biswas, S.; Banerjee, S.; Shlain, M. A.; Barfin, A. A.; Ulijn, R. V.; Nannenga, B. L.; Rappe, A. M.; Brauschweig, A. B. Photomechanochemical control over stereoselectivity in the [2 + 2] photodimerization of acenaphthylene. *Faraday Discuss.* **2023**, *241*, 266−277.

(26) Yan, D.; Wang, Z.; Zhang, Z. Stimuli-Responsive Crystalline Smart Materials: From Rational Design and Fabrication to Applications. *Acc. Chem. Res.* **2022**, *55*, 1047−1058.

(27) Wang, X.; Shan, M.; Zhang, S.; Chen, X.; Liu, W.; Chen, J.; Liu, W. Stimuli-Responsive Antibacterial Materials: Molecular Structures, Design Principles, and Biomedical Applications. *Adv. Sci.* **2022**, *9*, No. 2104843.

(28) Ramakrishnan, T.; Kumar, S. S.; Chelladurai, S. J. S.; Gnanasekaran, S.; Sivananthan, S.; Geetha, N. K.; Arthanari, R.; Assefa, G. B. Recent Developments in Stimuli Responsive Smart Materials and Applications: An Overview. *J. Nanomater.* **2022**, *2022*, No. e4031059.

(29) Hu, L.; Gao, Y.; Serpe, M. J. *Smart Stimuli-Responsive Polymers, Films, and Gels.*; John Wiley & Sons, 2022.

(30) Rivera-Tarazona, L. K.; Campbell, Z. T.; Ware, T. H. Stimuli-responsive engineered living materials. *Soft Matter* **2021**, *17*, 785−809.

(31) Kory, M. J.; Wörle, M.; Weber, T.; Payamyar, P.; van de Poll, S. W.; Dshemuchadse, J.; Trapp, N.; Schlüter, A. D. Gram-scale synthesis of two-dimensional polymer crystals and their structure analysis by X-ray diffraction. *Nat. Chem.* **2014**, *6*, 779−784.

(32) Morimoto, M.; Irie, M. Photochromism of diarylethene single crystals: crystal structures and photochromic performance. *Chem. Commun.* **2005**, 3895−3905.

(33) Kobatake, S.; Matsumoto, Y.; Irie, M. Conformational Control of Photochromic Reactivity in a Diarylethene Single Crystal. *Angew. Chem., Int. Ed.* **2005**, *44*, 2148−2151.

(34) Yang, L.; Wang, H.; Lang, M.; Peng, S. Recent Advances on High-Order Dipolar Annulations of Donor−Acceptor Cyclopropanes/Cyclobutanes. *Synthesis* **2024**, *56*, 389−398.
(35) Xia, Y.; Liu, X.; Feng, X. Asymmetric Catalytic Reactions of Donor−Acceptor Cyclopropanes. *Angew. Chem., Int. Ed.* **2021**, *60*, 9192−9204.
(36) Ivanova, O. A.; Trushkov, I. V. Donor-Acceptor Cyclopropanes in the Synthesis of Carbocycles. *Chem. Rec.* **2019**, *19*, 2189−2208.
(37) Budynina, E. M.; Ivanov, K. L.; Sorokin, I. D.; Melnikov, M. Y. Ring Opening of Donor−Acceptor Cyclopropanes with *N*-Nucleophiles. *Synthesis* **2017**, *49*, 3035−3068.
(38) Reissig, H.-U.; Hirsch, E. Donor-Acceptor Substituted Cyclopropanes: Synthesis and Ring Opening to 1,4-Dicarbonyl Compounds. *Chem. Rec.* **1980**, *19*, 813−814.
(39) Wenkert, E.; Alonso, M. E.; Buckwalter, B. L.; Chou, K. J. A method of synthesis of. beta.-methylfurans and. alpha.-methylene and. beta.-methylene. gamma.-lactones. Two menthofuran syntheses. *J. Am. Chem. Soc.* **1977**, *99*, 4778−4782.
(40) Jacob, A.; Oliver, G. A.; Werz, D. B. Understanding the Reactivity of Donor−Acceptor Cyclopropanes: Structural and Electronic Analysis. In *Donor Acceptor Cyclopropanes in Organic Synthesis*; John Wiley & Sons, Ltd, 2024; pp 15−36.
(41) Kreft, A.; Lücht, A.; Grunenberg, J.; Jones, P. G.; Werz, D. B. Kinetic Studies of Donor−Acceptor Cyclopropanes: The Influence of Structural and Electronic Properties on the Reactivity. *Angew. Chem., Int. Ed.* **2019**, *58*, 1955−1959.
(42) Masson, K.; Dousset, M.; Biletskyi, B.; Chentouf, S.; Naubron, J.-V.; Parrain, J.-L.; Commeiras, L.; Nava, P.; Chouraqui, G. Designing Donor-Acceptor Cyclopropane for the Thermal Synthesis of Carbocyclic Eight-Membered Rings. *Adv. Synth. Catal.* **2023**, *365*, 1002−1011.
(43) Liu, H.; Tian, L.; Wang, H.; Li, Z.-Q.; Zhang, C.; Xue, F.; Feng, C. A novel type of donor−acceptor cyclopropane with fluorine as the donor: (3 + 2)-cycloadditions with carbonyls. *Chem. Sci.* **2022**, *13*, 2686−2691.
(44) McKinnon, J. J.; Spackman, M. A.; Mitchell, A. S. Novel tools for visualizing and exploring intermolecular interactions in molecular crystals. *Acta Crystallogr., Sect. B: Struct. Sci.* **2004**, *60*, 627−668.
(45) McKinnon, J. J.; Jayatilaka, D.; Spackman, M. A. Towards quantitative analysis of intermolecular interactions with Hirshfeld surfaces. *Chem. Commun.* **2007**, 3814−3816.
(46) Van Der Spoel, D.; Lindhal, E.; Hess, B.; Groenhof, G.; Mark, A. E.; Berendsen, H. J. C. GROMACS: Fast, flexible, and free. *J. Comput. Chem.* **2005**, *26*, 1701−1718.
(47) Wang, J.; Wolf, R. M.; Caldwell, J. W.; Kollman, P. A.; Case, D. A. Development and testing of a general amber force field. *J. Comput. Chem.* **2004**, *25*, 1157−1174.
(48) Schmidt, L.; van der Spoel, D.; Walz, M.-M. Probing Phase Transitions in Organic Crystals Using Atomistic MD Simulations. *ACS Phys. Chem. Au* **2023**, *3*, 84−93.
(49) Gavezzotti, A.; Presti, L. L.; Rizzato, S. Molecular dynamics simulation of organic materials: structure, potentials and the MiCMoS computer platform. *CrystEngComm* **2022**, *24*, 922−930.
(50) Rizzato, S.; Gavezzotti, A.; Lo Presti, L. Molecular Dynamics Simulation of Molecular Crystals under Anisotropic Compression: Bulk and Directional Effects in Anthracene and Paracetamol. *Cryst. Growth Des.* **2020**, *20*, 7421−7428.
(51) Scheschkewitz, D. Comment on "Single-Crystal X-ray Structure of 1,3-Dimethylcyclobutadiene by Confinement in a Crystalline Matrix. *Science* **2010**, *330*, No. 1047.
(52) Alabugin, I. V.; Gold, B.; Shatruk, M.; Kovnir, K. Comment on "Single-Crystal X-ray Structure of 1,3-Dimethylcyclobutadiene by Confinement in a Crystalline Matrix. *Science* **2010**, *330*, No. 1047.